Published in final edited form as:
Crit Care Med. 2008 October ; 36(10): 2849–2857.

Ciglitazone ameliorates lung inflammation by modulating the IKK/NF-κB pathway following Hemorrhagic Shock

Ranjit S. Chima, **Paul W. Hake**, **Giovanna Piraino**, **Prajakta Mangeshkar**, **Alvin Denenberg**, and **Basilia Zingarelli**
Division of Critical Care Medicine, Cincinnati Children's Hospital Medical Center, University of Cincinnati College of Medicine, Cincinnati

Abstract

Objective—Peroxisome proliferator-activated receptor gamma (PPARγ) is a ligand-activated transcription factor. Ciglitazone a PPARγ ligand, has been shown to provide beneficial effects in experimental models of sepsis and ischemia/reperfusion injury. We investigated the effects of ciglitazone on lung inflammation following severe hemorrhage.

Design—Prospective, laboratory study, rodent model of hemorrhagic shock.

Setting—University hospital laboratory.

Subjects—Male Rats.

Interventions—Hemorrhagic shock was induced by withdrawing blood to a mean arterial pressure (MAP) of 50 mmHg. At 3 hours after hemorrhage, rats were rapidly resuscitated by returning their shed blood. At the time of resuscitation and every hour thereafter, animals received ciglitazone (10mg/kg) or vehicle intraperitoneally. Heart rate and MAP were measured throughout the experiment. Plasma and lung tissue were collected for analysis up to 3 hours after resuscitation.

Measurements and Main results—Ciglitazone treatment ameliorated MAP, reduced lung injury, significantly blunted lung neutrophil infiltration and lowered plasma interleukin -6 (IL-6), interleukin-10 (IL-10) and monocyte chemoattractant protein-1 (MCP-1) levels. In a time course analysis, vehicle-treated rats had a significant increase in nuclear factor-κB (NF-κB) DNA binding, which was preceded by increased inhibitor κB (IκB) protein kinase (IKK) activity and IκBα degradation in the lung. Treatment with ciglitazone significantly reduced IKK activity and IκBα degradation and completely inhibited NF-κB DNA binding. This reduction of IKK activity afforded by ciglitazone appeared to be a consequence of a physical interaction between PPARγ and IKK.

Conclusion—Ciglitazone ameliorates the inflammatory response and may reduce lung injury following hemorrhagic shock. These protective effects appear to be mediated through inhibition of the IKK/NF-κB pathway.

Keywords

Hemorrhage; Peroxisome proliferator-activated receptor-γ; Nuclear factor-κB; IκB kinase; Ciglitazone

Address for Correspondence: Basilia Zingarelli, M.D. Ph.D. Division of Critical Care Medicine Cincinnati Children's Hospital Medical Center 3333 Burnet Avenue, Cincinnati, OH 45229 Office: (513) 636-8704 basilia.zingarelli@cchmc.org.

INTRODUCTION

Unintentional injuries are the leading cause of death in the United States in individuals aged 1-44 years (1). Hemorrhage is the second most common cause of death in this age group, contributing to 30-40% of deaths (2). Additionally, hemorrhage accounts for the majority of early deaths following trauma (2, 3). The initial insult of trauma and/or hemorrhage sets up a systemic inflammatory response which, if uncontrolled, can lead to the development of multiple organ failure. Respiratory failure and lung injury are the most common and have been shown to play an important role in the further development of other organ failure (4, 5). The systemic inflammatory response is characterized by an overwhelming production of cytokines (IL-6, IL-10) and chemokines (MCP-1), which have been reported to play a key role in the pathogenesis of lung injury (6). There are no effective strategies to combat this systemic inflammatory state and the treatment is mainly supportive aimed at bleeding control and replenishing volume loss (1).

Peroxisome proliferator-activated receptor gamma (PPARγ) is a ligand activated transcription factor, which belongs to a family of nuclear receptors. It has a role in glucose homeostasis, atherosclerosis, adipocyte proliferation, cell cycle control and carcinogenesis (7). In addition, the PPARγ pathway plays a role in the inflammatory response (8, 9). PPARγ activation has been shown to have anti-inflammatory effects by repressing the expression of inflammatory response genes in activated macrophages and monocytes (10, 11).

Drugs belonging to the thiazolidinedione group, such as ciglitazone, are specific PPARγ ligands (12). *In vivo* treatment with these ligands has been shown to attenuate the organ injury associated with hemorrhagic shock, endotoxic shock and myocardial ischemia-reperfusion in rodents (13-16). However, in hemorrhagic shock the molecular mechanisms by which these ligands attenuate the inflammatory response has not been described.

Nuclear factor-κB (NF-κB) is a ubiquitous transcription factor. Under basal conditions, it exists in the cytosol in an inactive state bound to its physiologic inhibitor κBα (IκBα). Its activation requires removal and degradation of IκBα, an event that occurs after phosphorylation of IκB by a complex of IκB kinases (IKK). The IKK complex consists of three kinases, IKKα IKKβ and IKKγ Once phosphorylated, IκBα undergoes degradation allowing NF-κB to translocate to the nucleus where it regulates the expression of a variety of genes involved in the inflammatory process (17). It has been demonstrated that activation of NF-κB also plays a major role in the development of acute lung injury during the inflammatory response following hemorrhage (18-20).

Therefore, the purpose of this study was to investigate whether ciglitazone, a PPARγ ligand, would reduce the inflammatory response by modulating the NF-κB pathway in the lung following hemorrhagic shock.

MATERIALS AND METHODS

Rodent Model of Hemorrhagic Shock

The investigation conformed to the *Guide for the Care and Use of Laboratory Animals* published by the U.S. National Institutes of Health (NIH Publication No. 85-23, revised 1996) and commenced with the approval of the institutional Animal Care and Use Committee. Male Wistar rats (200-300 g, Charles River Laboratories, Wilmington MA) were anesthetized with pentobarbital (80 mg/kg) intraperitoneally (IP). The right femoral artery and left common carotid artery were cannulated (PE-50 tubing) and used for drawing blood and measuring mean arterial pressure (MAP), respectively. The trachea was

cannulated and all animals were placed on a rodent ventilator (Harvard Apparatus, Holliston, MA) with similar settings, tidal volume 7-8 ml/kg, rate 60 breaths/min and FiO2 of 0.4. Peak inspiratory pressure (PIP) was not measured and no positive endexpiratory pressure (PEEP) was applied. Hemorrhagic shock was induced as previously described (21). The animals were kept at a MAP of 50 mmHg for 3h by withdrawing or re-injecting blood through the femoral artery. At 3h rats were rapidly resuscitated over 10 min with their own shed blood supplemented with Ringer Lactate solution to a final volume equal to total shed blood and monitored for another 3h. Heart rates (HR) and MAP were measured using a pressure transducer and digitized using a Maclab A/D converter. This data was analyzed using Chart 5 software (AD Instruments Colorado Springs, CO) at 30 min intervals during the entire experiment.

Rats were randomly assigned to 3 groups- sham, vehicle, ciglitazone. Rats in the sham group underwent the surgical procedure, but were not bled. Rats in the vehicle and ciglitazone group received dimethyl sulphoxide (0.1 ml/kg DMSO IP) or ciglitazone (10 mg/kg IP) respectively at the time of resuscitation and hourly thereafter. The dose of ciglitazone was chosen on the basis of previous studies demonstrating anti-inflammatory effects in rodent models of critical illness (16, 22). Rats were sacrificed 1h, 2h and 3h following resuscitation. Lungs and plasma samples were collected from each rat and stored at -70°C.

Plasma Glucose levels and Lactate Levels

Glucose concentrations were measured using a commercially available quantitative colorimetric assay kit (BioAssay Systems, Hayward, CA), using the protocol recommended by the manufacturer. Lactate levels were measured using a quantitative colorimetric assay as described previously (23).

Plasma Cytokine and Chemokine Levels

Plasma levels of interleukin 6 (IL-6), interleukin 10 (IL-10) and monocyte chemoattractant protein (MCP-1) were determined by a multiplex array system (Linco-Research, St. Charles, MO).

Histopathological analysis

Lung tissue was fixed in 4% paraformaldehyde and embedded in paraffin. Sections were stained with hematoxylin eosin stain. These sections were evaluated by light microscopy for evidence of lung injury.

Lung Myeloperoxidase Activity

Myeloperoxidase activity was determined as an index of neutrophil accumulation in lung homogenates collected from the rats as previously described (16).

Subcellular Fractionation and Nuclear Protein Extraction

Lung samples were homogenized with a Polytron homogenizer (Brinkmann Instruments, West Orange, NY) in a buffer containing 0.32 M sucrose, 10 mM Tris-HCl (pH 7.4), 1 mM EGTA, 2 mM EDTA, 5 mM NaN3, 10 mM β-mercaptoethanol, 20 μM leupeptin, 0.15 μM pepstatin A, 0.2 mM PMSF, 50 mM NaF, 1 mM sodium orthovanadate, and 0.4 nM microcystin. The homogenates were centrifuged (1,000 × g, 10 min), and the supernatant (cytosol plus membrane extract) was collected. The pellets were solubilized in Triton buffer (1% Triton X-100, 150 mM NaCl, 10 mM Tris-HCl (pH 7.4), 1 mM EGTA, 1 mM EDTA, 0.2 mM sodium orthovanadate, 20 μM leupeptin A, and 0.2 mM PMSF). The lysates were centrifuged (15,000 × g, 30 min, 4°C), and the supernatant (nuclear extract) was collected.

Western blot analysis for IκBα

The cytosol degradation of IκBα in the lung was determined by immunoblot analyses in cytosol extracts using primary antibody against IκBα. Immunoreaction was visualized by chemiluminescence and on a photographic film. Densitometric analysis of blots was performed using ImageQuant (Molecular Dynamics, Sunnyvale, CA).

Electrophoretic Mobility Shift Assay for NF-κB

Electrophoretic mobility shift assays were performed as previously described (24). Oligonucleotide probes corresponding to the NF-κB consensus sequence (5′-AGT TGA GGG GAC TTT CCC AGG C-3′) were labeled with [γ-^{32}P] ATP using T4 polynucleotide kinase and were purified in Bio-Spin chromatography columns (Bio-Rad, Hercules, CA). Twenty five micrograms of nuclear protein were preincubated with EMSA buffer (12 mM HEPES (pH 7.9), 4 mM Tris-HCl (pH 7.9), 25 mM KCl, 5 mM $MgCl_2$, 1 mM EDTA, 1 mM DTT, 50 ng/ml poly(d(I-C)), 12% glycerol (v/v), and 0.2 mM PMSF) on ice for 10 min before addition of the radiolabeled oligonucleotide for an additional 10 min. The specificity of the binding reaction was determined by co-incubating the samples with 10 fold excess of unlabeled oligonucleotide (competition assay) or anti-p65 antibody (supershift assay). Protein-nucleic acid complexes were resolved using a nondenaturing polyacrylamide gel consisting of 5% acrylamide (29/1 ratio of acrylamide/bisacrylamide) and were run in 0.5x TBE (45 mM Tris-HCl, 45 mM boric acid, and 1 mM EDTA) for 1 h at constant current (30 mA). Gels were transferred to Whatman 3M paper (Clifton, NJ), dried under a vacuum at 80°C for 1 h, and exposed to photographic film at -70°C with an intensifying screen. Densitometric analysis was performed using ImageQuant (Molecular Dynamics, Sunnyvale, CA).

Assay of IKK activitiy

IKK activity was determined by immune complex kinase assay and was estimated as the ability to phosphorylate GST-IκBα as previously described (24). After immunoprecipitation of lysate with specific Ab directed to IKKγ, the immunoprecipitate was incubated for 30 min at 30°C in 40 μl of reaction buffer (25 mM HEPES (pH 7.6), 20 mM $MgCl_2$, 20 mM glycerol phosphate, 0.1 mM sodium orthovanadate, 2 mM DTT, 25 μM ATP, and 5 μCi [γ-^{32}P]ATP). GST- $I\kappa B\alpha_{1–54}$ (4 μg) was used as substrate for the IKK complex. Reaction products were separated by SDS-PAGE and visualized by autoradiography. Densitometric analysis was performed using ImageQuant (Molecular Dynamics, Sunnyvale, CA).

Immunoprecipitation

Cytosolic extracts were immunoprecipitated with primary antibody against IKKγ with protein AG-sepharose beads overnight at 4°C. The immune complexes were separated electrophoretically in a 10% Tris-glycine gel and transferred to a nitrocellulose membrane. For immunoblotting, membranes were incubated with primary antibody against PPARγ. To assess loading, membranes were also incubated with antibody against IKKγ. Densitometric analysis of the blots was performed using ImageQuant (Molecular Dynamics, Sunnyvale, CA).

Materials

The primary antibodies directed against IκBα, IKKγ, p65 and oligonucleotide corresponding to NF-κB consensus sequence were obtained form Santa Cruz Biotechnology (Santa Cruz, CA). The primary antibody against PPARγ was obtained from Affinity Bioreagents (Golden, CO). Ciglitazone was obtained from Biomol (Plymouth Meeting, PA). All other chemicals were purchased from Sigma-Aldrich (St. Louis, MO).

Data Analysis

Data was analyzed using SigmaStat for Windows Version 3.10 (SysStat Software, San Jose, CA). MAP values are expressed as mean ± SD; the remainder of the values in the figures and text are expressed as mean ± SEM of n observations, where n represents the number of animals in each group. Specifically, MAP results were analyzed using a general linear model for repeated measures allowing for missing data. For the remainder of the data analysis a two factor ANOVA or a one way ANOVA followed by Bonferroni correction was utilized. A value of $p < 0.05$ was considered significant.

RESULTS

Effect of Ciglitazone on MAP and Plasma Lactate Levels

Both ciglitazone and vehicle-treated rats had similar MAP at baseline (122.55±8 vs. 127.41±13.6 mmHg) and during hemorrhagic shock (52±1.4 vs. 51.7±0.7 mmHg) (Fig. 1). Rats in both groups underwent the same degree of hemorrhage (ciglitazone 49.7±5% vs. vehicle 48.8±3.11 % total blood volume). At 1h, 2h and 3h following resuscitation ciglitazone-treated rats had significantly higher MAP compared to vehicle-treated rats (Fig. 1). At the end of the experiment, ciglitazone-treated rats had higher MAP (89.5±9.2 mmHg) when compared to vehicle-treated (69.4±17.8 mmHg; $p < 0.05$). At 1h following resuscitation, plasma lactate levels were significantly lower in the ciglitazone-treated rats when compared to the vehicle-treated group (8.51±2.53 vs. 1.67±0.13 μmol/ml, $p < 0.05$) (Fig. 2).

Effect of Ciglitazone on Plasma Cytokine and Chemokine Levels

Plasma IL-6, IL-10 and MCP-1 levels were measured at 1h, 2h and 3h following resuscitation. Vehicle-treated rats had a significant increase in cytokine and chemokine levels following resuscitation when compared to rats that underwent sham surgery (Fig. 3). In contrast, ciglitazone treatment attenuated this increase in cytokine and chemokine levels following resuscitation (Fig. 3).

Effect of Ciglitazone on Plasma Glucose Levels

Since thiazolidinediones are commonly used as oral hypoglycemic agents, we tested whether ciglitazone might have an effect on glucose levels. Glucose levels in rats that underwent sham surgery were 157±5.8 mg/dl. At the end of hemorrhage and resuscitation, plasma glucose levels were 118±21.8 mg/dl in vehicle-treated rats and 177±28.4 mg/dl in ciglitazone-treated rats.

Effect of Ciglitazone of Lung Histopathology

Following hemorrhage and resuscitation vehicle-treated rats had a significant alteration of lung architecture as demonstrated by alveolar disruption, interstitial swelling and inflammatory cell infiltration when compared to sham rats (Fig. 4). Also notable was the margination of neutrophils along the walls of pulmonary blood vessels. In contrast, ciglitazone-treatment attenuated the changes in lung architecture and inflammatory cell infiltration (Fig. 4).

Effect of Ciglitazone on Lung Neutrophil Infiltration

Following severe hemorrhage and shock, multiple organ failure is a serious complication and is characterized by the accumulation of neutrophils in various organs. The lung is one of the organs predominantly affected. We evaluated lung neutrophil infiltration by measuring myeloperoxidase activity at 1h, 2h and 3h following resuscitation. Vehicle and ciglitazone-treated rats had a significant increase in myeloperoxidase activity following resuscitation

when compared to rats that underwent sham surgery (Fig. 5). However, ciglitazone-treated rats had significantly lower myeloperoxidase activity at 1h, 2h and 3h following resuscitation when compared to vehicle-treated rats (Fig. 5).

Effect of Ciglitazone on the NF-κB pathway in the Lung

Since NF-κB represents a major transcription factor implicated in the inflammatory response, we investigated the effect of ciglitazone on NF-κB DNA binding in the lung. In a time-course EMSA, vehicle-treated rats had an increase in NF-κB DNA binding following resuscitation. By densitometric analysis, this increase was most notable at 1h following resuscitation and declined thereafter. In contrast, ciglitazone-treated rats did not have any increase in NF-κB DNA binding following resuscitation (Fig. 6).

Since activation of IKK followed by IκBα degradation is a prerequisite for the nuclear translocation and DNA binding of NF-κB, we determined IKK activity and IκBα degradation in the cytosol. In a time-course analysis, vehicle-treated rats had increased IκBα degradation at 1h after resuscitation followed by progressive replenishment of IκBα content (Fig. 6). This was associated with increased activity of IKK as early as 1h after resuscitation (Fig. 6). In a similar time-course analysis, ciglitazone treatment inhibited degradation of IκBα and activity of IKK (Fig. 7).

Effect of Ciglitazone on IKK and PPARγ Interaction in the Lung

Since the inhibitory effects of ciglitazone treatment following resuscitation on the NF-κB pathway appeared to be a consequence of altered IKK activity in the cytosol, we investigated the mechanism by which PPARγ may inhibit IKK. To this aim, we investigated whether there was a physical association between IKK and PPARγ. To demonstrate this, lung cytosol fraction was immunoprecipitated with an antibody against IKKγ and, subsequently, probed with an antibody to PPARγ. Interestingly, we observed a constitutive physical association between IKK and PPARγ at basal levels, i.e. in sham rats (Fig. 8). At 1h after resuscitation, there seemed to be a decrease in IKK and PPARγ association in the vehicle-treated rats (Fig. 8). In contrast, treatment with ciglitazone maintained this PPARγ/IKK interaction (Fig. 8).

DISCUSSION

The beneficial role of PPARγ ligands in reducing organ injury in an *in vivo* model of hemorrhagic shock has been demonstrated previously (13). Our study represents the first investigation to elucidate the molecular mechanisms by which ciglitazone, a PPARγ ligand, modulates the inflammatory response following hemorrhagic shock in a rodent. In our model treatment with ciglitazone, when given following hemorrhage, ameliorated MAP and blunted the inflammatory response as evidenced by a reduction in cytokine and chemokine levels. Treatment with ciglitazone also reduced lung neutrophil infiltration, that was associated with a reduction in nuclear NF-κB DNA binding.

Ciglitazone treatment ameliorated hypotension following resuscitation when compared to vehicle-treated rats, as evidenced by significantly higher MAP during the resuscitation phase. Similar to our study, in a rodent model of hemorrhagic shock 15d-PGJ_2 has been shown to exert a positive effect on blood pressure (13). This amelioration of blood pressure following administration of PPARγ ligands has been shown in other models of inflammation such as polymicrobial sepsis and myocardial ischemia/reperfusion (16, 25). Of note, ciglitazone when administered to normal rats does not have any effects on blood pressure (16). Therefore, the hemodynamic effect of ciglitazone may be linked to the drug's ability to resolve the inflammatory response. Nevertheless, we cannot exclude other

mechanistic effects for the improvement of blood pressure in ciglitazone-treated rats. For example, PPARγ activation has been shown to ameliorate contractile function by improving glucose utilization and cardiac energetics in the myocardium of diabetic animals (26).

Plasma lactate is a commonly used marker as an endpoint for resuscitation for patients in shock. Additionally, both initial lactate levels and the duration of hyperlactatemia have been shown to correlate with organ failure in trauma patients (27, 28). The most likely cause of hyperlactatemia following hemorrhage appears to be epinephrine mediated upregulation of lactate production from skeletal muscle (29, 30). In our study, ciglitazone-treated rats had significantly lower lactate levels when compared to vehicle-treated rats at 1h following resuscitation; while, thereafter, lactate levels declined similarly in both groups. The exact mechanism for the observed difference in lactate levels at 1h following resuscitation with ciglitazone is unclear. However, since PPARγ has an important role in glucose homeostasis, it is possible that ciglitazone treatment causes better glucose utilization and metabolism or improved hepatic clearance. For example, in a model of myocardial ischemia/reperfusion administration of another thiazolidinedione, troglitazone, has been shown to improve lactate clearance by increased myocardial uptake (25). Additionally, therapeutic approaches with insulin in hemorrhagic shock have been shown to improve hepatic energetics (31).

In addition to modulation of glucose metabolism, PPARγ has been shown to be a negative regulator of the inflammatory response (8). For example, PPARγ ligands have been shown to suppress cytokine production and macrophage activation *in vitro* (10, 11). Similar results have been demonstrated in models of polymicrobial sepsis and ischemia/reperfusion injury *in vivo* (16, 32). Interestingly, the anti-inflammatory effects of PPARγ ligands appear to be related to inhibition of signal transduction pathways independent of their effects on glucose metabolism. Hemorrhagic shock sets up a systemic inflammatory response that is characterized by the production of cytokines and chemokines. In comparison to vehicle treatment ciglitazone reduced the severity of this response. Ciglitazone-treated animals had lower plasma levels of pro-inflammatory mediators IL-6 and MCP-1. Interestingly, treatment with ciglitazone also reduced plasma levels of IL-10. Although this cytokine has been reported to function as an anti-inflammatory mediator, several clinical studies have demonstrated that IL-10 levels correlate closely with severity of injury (33, 34). On the contrary, similarly to our findings, several experimental studies have demonstrated that amelioration of organ function and reduction of systemic inflammation is associated with a decrease in IL-10 levels (35, 36).

Lung injury is a major consequence of hemorrhagic shock; neutrophils being a major cell type incriminated in this response (37). Ciglitazone-treated animals had reduction in lung neutrophil infiltration following resuscitation when compared to vehicle-treated animals. In support of our current findings, other PPARγ ligands, including ciglitazone, have been shown to suppress neutrophil responses to chemotactic factors and to modulate endothelial cell expression of adhesion molecules *in vitro*. Additionally, PPARγ ligands have been shown to reduce lung neutrophil infiltration during polymicrobial sepsis and ischemia-reperfusion injury *in vivo* (14, 16, 38-41). In our study we also demonstrated a reduction in plasma MCP-1 levels after ciglitazone treatment. However, we did not measure levels of the keratinocyte-derived chemokine (KC), a major chemokine that is involved in neutrophil trafficking. Nevertheless, there is experimental evidence that MCP-1 may participate in neutrophil accumulation in distant organs by regulating KC production during trauma-hemorrhage (42). Although, the exact link between the cytokine/chemokine responses and lung neutrophil infiltration in our study is not completely defined, our data suggest that reduction in MCP-1 production after ciglitazone treatment may contribute to a reduction in lung neutrophil infiltration.

Activation of the NF-κB pathway has been shown to occur early following both hemorrhage and resuscitation, and play a major role in lung injury (19, 43). In our study, NF-κB DNA binding increased in the lung 1h after resuscitation in vehicle-treated rats, whereas ciglitazone treatment prevented this increase. The inhibitory effect of ciglitazone on NF-κB appeared to be secondary to inhibition at the cytosol level of the kinase, IKK. Although PPARγ ligands, such as 15d PGJ_2, have been described to have a direct PPARγ–independent effect on IKK (44); ciglitazone has not been demonstrated to have a similar effect. On the other hand, PPARγ has been demonstrated to directly affect mitogen-activated protein kinases. For example, in a murine model of colitis PPARγ heterozygous mice had a reduction in phosphorylation of c-Jun amino-terminal kinase (JNK) and p38 (45). Similarly, a recent study using an adipocyte cell line demonstrated inhibition of JNK by rosiglitazone and these effects were PPARγ mediated (46). Additionally, kinases have been demonstrated to physically interact with PPARγ. In a recent study, MEK has been shown to downregulate PPARγ by direct interaction in human embryonic kidney cells (47). In our study, we demonstrated that at basal normal conditions PPARγ interacted with IKK in the lung. This physical association was paralleled by reduced kinase activity. After hemorrhage and resuscitation, a reduction of this PPARγ/IKK complex correlated with high IKK activity. Ciglitazone treatment restored this PPARγ/IKK interaction. Our study is the first to demonstrate such an effect of PPARγ on the NF-κB signaling pathway *in vivo*. There is some data to suggest the plausibility of this finding. Firstly, the cytosolic localization of PPARγ, a nuclear receptor, has been previously demonstrated (48, 49). Additionally, there is evidence that interaction of PPARγ with a kinase, such as MEK may cause translocation of PPARγ from the nucleus to the cytosol (47). Our immunoprecipitation experiments attempted to define the mechanism by which ciglitazone might inhibit IKK during hemorrhagic shock; however, the exact nature of this protein complex is unclear. Whether other proteins such as phosphatases or kinases may be involved needs to be further investigated. Also, we cannot exclude the possibility of PPARγ inhibiting NF-κB signaling at a nuclear level. PPARγ has been shown to directly transrepress NF-κB in a DNA-binding independent manner. These actions may be mediated through binding of co-activators or directly binding to NF-κB subunits p65 and p50 (50, 51). Further studies would be needed to elucidate the exact molecular mechanisms by which PPARγ inhibits the NF-κB pathway in the lung following severe hemorrhage and resuscitation.

Our study has some limitations. There is considerable variation in cytokine and chemokine levels following resuscitation even in consideration of remarkable NF-κB inhibition. Although gene expression of these mediators may be mediated by NF-κB activation, we cannot exclude that other cellular complex mechanisms may regulate protein synthesis and therefore final content, such as mRNA stability and turnover. Whether ciglitazone may also affect these processes is not known. Our choice of ciglitazone, as a PPARγ ligand, in this study was based on previous studies demonstrating *in vivo* anti-inflammatory effects (16, 22). Whether other PPARγ ligands would have similar effects in hemorrhagic shock has not yet been investigated. For clinical relevance, additional PPARγ ligands with different structures would need to be studied.

CONCLUSION

Our current study represents the first to explore the possible molecular mechanisms by which ciglitazone, a PPARγ ligand, ameliorates the inflammatory response in the lung following severe hemorrhage. These protective effects appear to be mediated through inhibition of the pro-inflammatory NF-κB pathway. Of clinical relevance, the effects of ciglitazone were demonstrated when given as a treatment following hemorrhagic shock.

Since thiazolidinediones are currently FDA approved for human use, other drugs belonging to this group may represent a therapeutic option in treating trauma/shock conditions.

Acknowledgments

This study was supported by the National Institutes of Health (R01 GM-67202, R01 AG-27990 and 5T32 GM008478-14)

BIBLIOGRAPHY

1. Kauvar DS, Wade CE. The epidemiology and modern management of traumatic hemorrhage: US and international perspectives. Crit Care. 2005; 9(Suppl 5):S1–9. [PubMed: 16221313]
2. Sauaia A, Moore FA, Moore EE, et al. Epidemiology of trauma deaths: a reassessment. J Trauma. 1995; 38:185–193. [PubMed: 7869433]
3. Acosta JA, Yang JC, Winchell RJ, et al. Lethal injuries and time to death in a level I trauma center. J Am Coll Surg. 1998; 186:528–533. [PubMed: 9583692]
4. Durham RM, Moran JJ, Mazuski JE, et al. Multiple organ failure in trauma patients. J Trauma. 2003; 55:608–616. [PubMed: 14566110]
5. Ciesla DJ, Moore EE, Johnson JL, et al. The role of the lung in postinjury multiple organ failure. Surgery. 2005; 138:749–757. discussion 757-748. [PubMed: 16269305]
6. Bhatia M, Moochhala S. Role of inflammatory mediators in the pathophysiology of acute respiratory distress syndrome. J Pathol. 2004; 202:145–156. [PubMed: 14743496]
7. Rocchi S, Auwerx J. Peroxisome proliferator-activated receptor-gamma: a versatile metabolic regulator. Ann Med. 1999; 31:342–351. [PubMed: 10574507]
8. Zingarelli B, Cook JA. Peroxisome proliferator-activated receptor-gamma is a new therapeutic target in sepsis and inflammation. Shock. 2005; 23:393–399. [PubMed: 15834303]
9. Abdelrahman M, Sivarajah A, Thiemermann C. Beneficial effects of PPAR-gamma ligands in ischemia-reperfusion injury, inflammation and shock. Cardiovasc Res. 2005; 65:772–781. [PubMed: 15721857]
10. Jiang C, Ting AT, Seed B. PPAR-gamma agonists inhibit production of monocyte inflammatory cytokines. Nature. 1998; 391:82–86. [PubMed: 9422509]
11. Ricote M, Li AC, Willson TM, et al. The peroxisome proliferator-activated receptor-gamma is a negative regulator of macrophage activation. Nature. 1998; 391:79–82. [PubMed: 9422508]
12. Willson TM, Lehmann JM, Kliewer SA. Discovery of ligands for the nuclear peroxisome proliferator-activated receptors. Ann N Y Acad Sci. 1996; 804:276–283. [PubMed: 8993550]
13. Abdelrahman M, Collin M, Thiemermann C. The peroxisome proliferator-activated receptor-gamma ligand 15-deoxyDelta12,14 prostaglandin J2 reduces the organ injury in hemorrhagic shock. Shock. 2004; 22:555–561. [PubMed: 15545828]
14. Kaplan JM, Cook JA, Hake PW, et al. 15-Deoxy-delta(12,14)-prostaglandin J(2) (15D-PGJ(2)), a peroxisome proliferator activated receptor gamma ligand, reduces tissue leukosequestration and mortality in endotoxic shock. Shock. 2005; 24:59–65. [PubMed: 15988322]
15. Ito H, Nakano A, Kinoshita M, et al. Pioglitazone, a peroxisome proliferator-activated receptor-gamma agonist, attenuates myocardial ischemia/reperfusion injury in a rat model. Lab Invest. 2003; 83:1715–1721. [PubMed: 14691289]
16. Zingarelli B, Sheehan M, Hake PW, et al. Peroxisome proliferator activator receptor-gamma ligands, 15-deoxy-Delta(12,14)-prostaglandin J2 and ciglitazone, reduce systemic inflammation in polymicrobial sepsis by modulation of signal transduction pathways. J Immunol. 2003; 171:6827–6837. [PubMed: 14662889]
17. Zingarelli B. Nuclear factor-kappaB. Crit Care Med. 2005; 33:S414–416. [PubMed: 16340408]
18. Fan J, Ye RD, Malik AB. Transcriptional mechanisms of acute lung injury. Am J Physiol Lung Cell Mol Physiol. 2001; 281:L1037–1050. [PubMed: 11597894]
19. Shenkar R, Abraham E. Hemorrhage induces rapid in vivo activation of CREB and NF-kappaB in murine intraparenchymal lung mononuclear cells. Am J Respir Cell Mol Biol. 1997; 16:145–152. [PubMed: 9032121]

20. Schwartz MD, Moore EE, Moore FA, et al. Nuclear factor-kappa B is activated in alveolar macrophages from patients with acute respiratory distress syndrome. Crit Care Med. 1996; 24:1285–1292. [PubMed: 8706481]
21. Zingarelli B, Ischiropoulos H, Salzman AL, et al. Amelioration by mercaptoethylguanidine of the vascular and energetic failure in haemorrhagic shock in the anesthetised rat. Eur J Pharmacol. 1997; 338:55–65. [PubMed: 9408003]
22. Zingarelli B, Hake PW, Mangeshkar P, et al. Diverse cardioprotective signaling mechanisms of peroxisome proliferator-activated receptor-gamma ligands, 15-deoxy-Delta12,14-prostaglandin J2 and ciglitazone, in reperfusion injury: role of nuclear factor-kappaB, heat shock factor 1, and Akt. Shock. 2007; 28:554–563. [PubMed: 17589386]
23. Gutman, I.; Wahlefeld, A. L-Lactate; Determination with lactic dehydrogenase and NAD.. In: Bergmeyer, H., editor. Methods of Enzymatic Analysis. 2nd.. Academic Press Inc.; New York: 1974. p. 1461-1468.
24. Zingarelli B, Hake PW, Yang Z, et al. Absence of inducible nitric oxide synthase modulates early reperfusion-induced NF-kappaB and AP-1 activation and enhances myocardial damage. Faseb J. 2002; 16:327–342. [PubMed: 11874982]
25. Zhu P, Lu L, Xu Y, et al. Troglitazone improves recovery of left ventricular function after regional ischemia in pigs. Circulation. 2000; 101:1165–1171. [PubMed: 10715264]
26. Golfman LS, Wilson CR, Sharma S, et al. Activation of PPARgamma enhances myocardial glucose oxidation and improves contractile function in isolated working hearts of ZDF rats. Am J Physiol Endocrinol Metab. 2005; 289:E328–336. [PubMed: 15797988]
27. Manikis P, Jankowski S, Zhang H, et al. Correlation of serial blood lactate levels to organ failure and mortality after trauma. Am J Emerg Med. 1995; 13:619–622. [PubMed: 7575797]
28. Blow O, Magliore L, Claridge JA, et al. The golden hour and the silver day: detection and correction of occult hypoperfusion within 24 hours improves outcome from major trauma. J Trauma. 1999; 47:964–969. [PubMed: 10568731]
29. Luchette FA, Jenkins WA, Friend LA, et al. Hypoxia is not the sole cause of lactate production during shock. J Trauma. 2002; 52:415–419. [PubMed: 11901313]
30. James JH, Luchette FA, McCarter FD, et al. Lactate is an unreliable indicator of tissue hypoxia in injury or sepsis. Lancet. 1999; 354:505–508. [PubMed: 10465191]
31. Chang CG, Van Way CW 3rd, Dhar A, et al. The use of insulin and glucose during resuscitation from hemorrhagic shock increases hepatic ATP. J Surg Res. 2000; 92:171–176. [PubMed: 10896818]
32. Cuzzocrea S, Pisano B, Dugo L, et al. Rosiglitazone and 15-deoxy-Delta12,14-prostaglandin J2, ligands of the peroxisome proliferator-activated receptor-gamma (PPAR-gamma), reduce ischaemia/reperfusion injury of the gut. Br J Pharmacol. 2003; 140:366–376. [PubMed: 12970094]
33. Hensler T, Sauerland S, Bouillon B, et al. Association between injury pattern of patients with multiple injuries and circulating levels of soluble tumor necrosis factor receptors, interleukin-6 and interleukin-10, and polymorphonuclear neutrophil elastase. J Trauma. 2002; 52:962–970. [PubMed: 11988666]
34. Neidhardt R, Keel M, Steckholzer U, et al. Relationship of interleukin-10 plasma levels to severity of injury and clinical outcome in injured patients. J Trauma. 1997; 42:863–870. discussion 870-861. [PubMed: 9191668]
35. Marcu AC, Paccione KE, Barbee RW, et al. Androstenetriol immunomodulation improves survival in a severe trauma hemorrhage shock model. J Trauma. 2007; 63:662–669. [PubMed: 18073617]
36. Levy RM, Mollen KP, Prince JM, et al. Systemic inflammation and remote organ injury following trauma require HMGB1. Am J Physiol Regul Integr Comp Physiol. 2007; 293:R1538–1544. [PubMed: 17652366]
37. Abraham E. Neutrophils and acute lung injury. Crit Care Med. 2003; 31:S195–199. [PubMed: 12682440]
38. Ito K, Shimada J, Kato D, et al. Protective effects of preischemic treatment with pioglitazone, a peroxisome proliferator-activated receptor-gamma ligand, on lung ischemia-reperfusion injury in rats. Eur J Cardiothorac Surg. 2004; 25:530–536. [PubMed: 15037267]

39. Pasceri V, Wu HD, Willerson JT, et al. Modulation of vascular inflammation in vitro and in vivo by peroxisome proliferator-activated receptor-gamma activators. Circulation. 2000; 101:235–238. [PubMed: 10645917]
40. Imamoto E, Yoshida N, Uchiyama K, et al. Inhibitory effect of pioglitazone on expression of adhesion molecules on neutrophils and endothelial cells. Biofactors. 2004; 20:37–47. [PubMed: 15096659]
41. Standiford TJ, Keshamouni VG, Reddy RC. Peroxisome proliferator-activated receptor-{gamma} as a regulator of lung inflammation and repair. Proc Am Thorac Soc. 2005; 2:226–231. [PubMed: 16222042]
42. Frink M, Lu A, Thobe BM, et al. Monocyte chemoattractant protein-1 influences trauma-hemorrhage-induced distal organ damage via regulation of keratinocyte-derived chemokine production. Am J Physiol Regul Integr Comp Physiol. 2007; 292:R1110–1116. [PubMed: 17095647]
43. Altavilla D, Saitta A, Squadrito G, et al. Evidence for a role of nuclear factor-kappaB in acute hypovolemic hemorrhagic shock. Surgery. 2002; 131:50–58. [PubMed: 11812963]
44. Straus DS, Pascual G, Li M, et al. 15-deoxy-delta 12,14-prostaglandin J2 inhibits multiple steps in the NF-kappa B signaling pathway. Proc Natl Acad Sci U S A. 2000; 97:4844–4849. [PubMed: 10781090]
45. Desreumaux P, Dubuquoy L, Nutten S, et al. Attenuation of colon inflammation through activators of the retinoid X receptor (RXR)/peroxisome proliferator-activated receptor gamma (PPARgamma) heterodimer. A basis for new therapeutic strategies. J Exp Med. 2001; 193:827–838. [PubMed: 11283155]
46. Diaz-Delfin J, Morales M, Caelles C. Hypoglycemic action of thiazolidinediones/peroxisome proliferator-activated receptor gamma by inhibition of the c-Jun NH2-terminal kinase pathway. Diabetes. 2007; 56:1865–1871. [PubMed: 17416798]
47. Burgermeister E, Chuderland D, Hanoch T, et al. Interaction with MEK causes nuclear export and downregulation of peroxisome proliferator-activated receptor gamma. Mol Cell Biol. 2007; 27:803–817. [PubMed: 17101779]
48. Shibuya A, Wada K, Nakajima A, et al. Nitration of PPARgamma inhibits ligand-dependent translocation into the nucleus in a macrophage-like cell line, RAW 264. FEBS Lett. 2002; 525:43–47. [PubMed: 12163159]
49. Thuillier P, Baillie R, Sha X, et al. Cytosolic and nuclear distribution of PPARgamma2 in differentiating 3T3-L1 preadipocytes. J Lipid Res. 1998; 39:2329–2338. [PubMed: 9831621]
50. Li M, Pascual G, Glass CK. Peroxisome proliferator-activated receptor gamma-dependent repression of the inducible nitric oxide synthase gene. Mol Cell Biol. 2000; 20:4699–4707. [PubMed: 10848596]
51. Chung SW, Kang BY, Kim SH, et al. Oxidized low density lipoprotein inhibits interleukin-12 production in lipopolysaccharide-activated mouse macrophages via direct interactions between peroxisome proliferator-activated receptor-gamma and nuclear factor-kappa B. J Biol Chem. 2000; 275:32681–32687. [PubMed: 10934192]

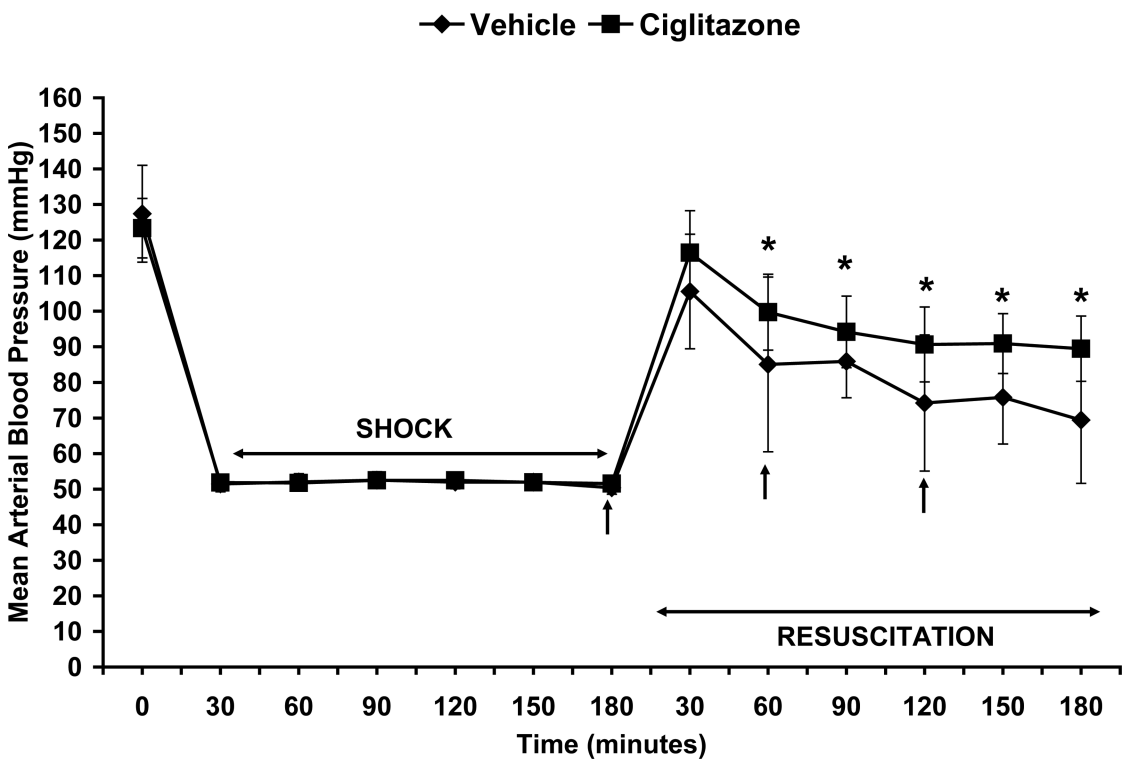

Figure 1. Effect of *in vivo* treatment with vehicle (DMSO) or ciglitazone on MAP in rats subjected to hemorrhage and resuscitation

Following resuscitation, in the vehicle group n=10, 7, 4 rats at 1h, 2h and 3h respectively. Following resuscitation, in the ciglitazone group n=15, 10, 5 rats at 1h, 2h and 3h respectively. Each data point represents the mean ± SD of 4 to 10 rats in the vehicle-group and 5 to 15 rats in the ciglitazone-treated group. Vehicle (DMSO) or ciglitazone (10 mg/kg) was administered IP at resuscitation and hourly thereafter. Arrows indicate time of ciglitazone or vehicle administration. *$p < 0.05$ vs. vehicle treated rats.

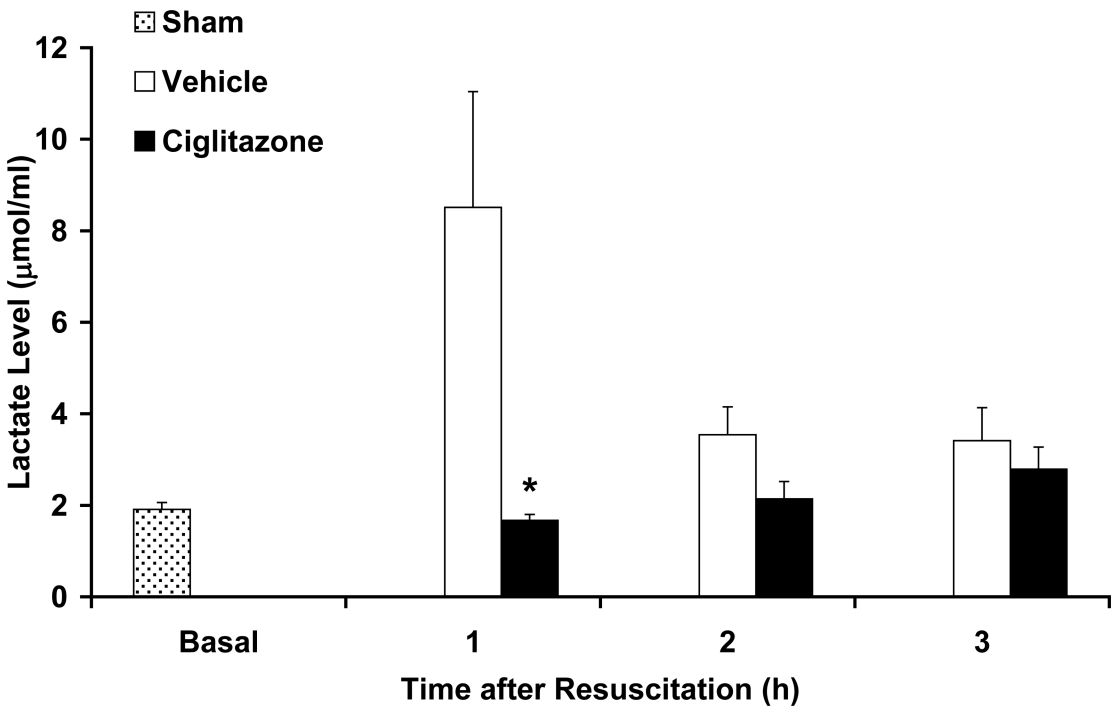

Figure 2. Effect of *in vivo* treatment with vehicle (DMSO) or ciglitazone on plasma lactate levels (µmol/ml) in rats subjected to hemorrhage and resuscitation

Each data point represents the mean ± SEM of 3 to 5 rats. Basal level represents level in sham rats, $*p < 0.05$ vs. vehicle treated rats.

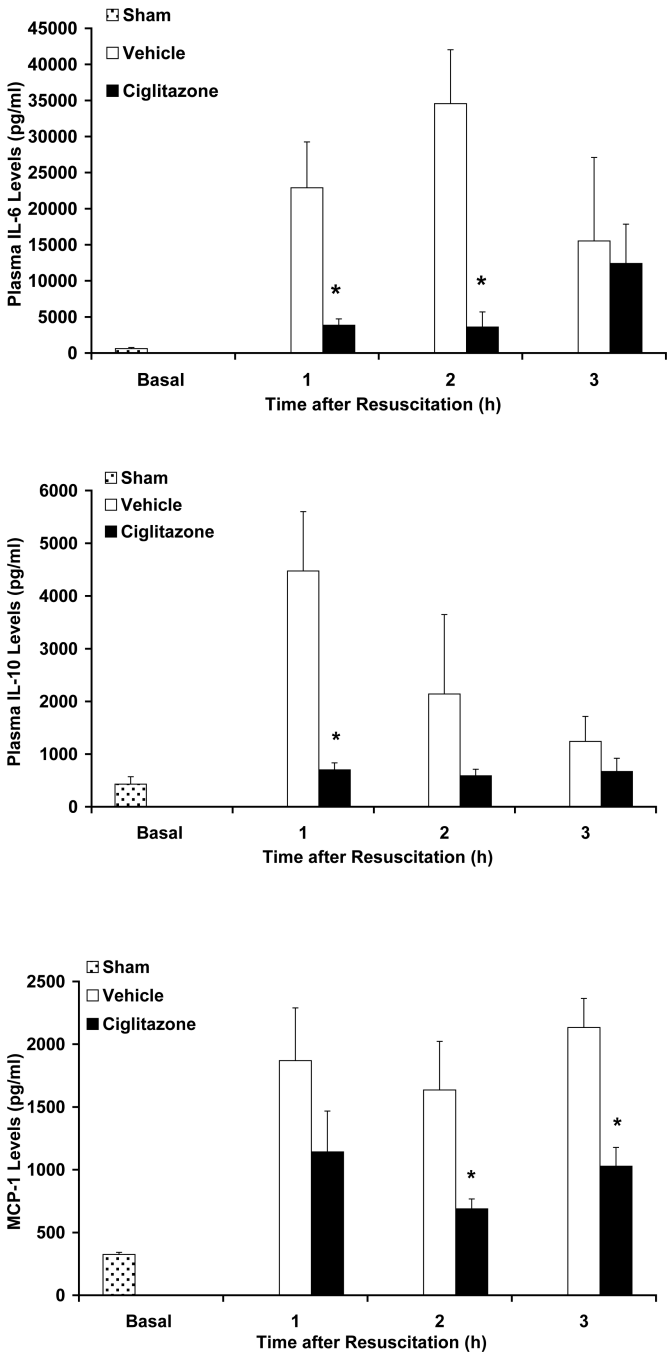

Figure 3. Effect of *in vivo* treatment with vehicle (DMSO) or ciglitazone on plasma levels of IL-6, IL-10 and MCP-1 (pg/ml) in rats subjected to hemorrhage and resuscitation

Each data point represents the mean ± SEM of 3 to 5 rats. Basal level represents level in sham rats, $*p < 0.05$ vs. vehicle-treated rats.

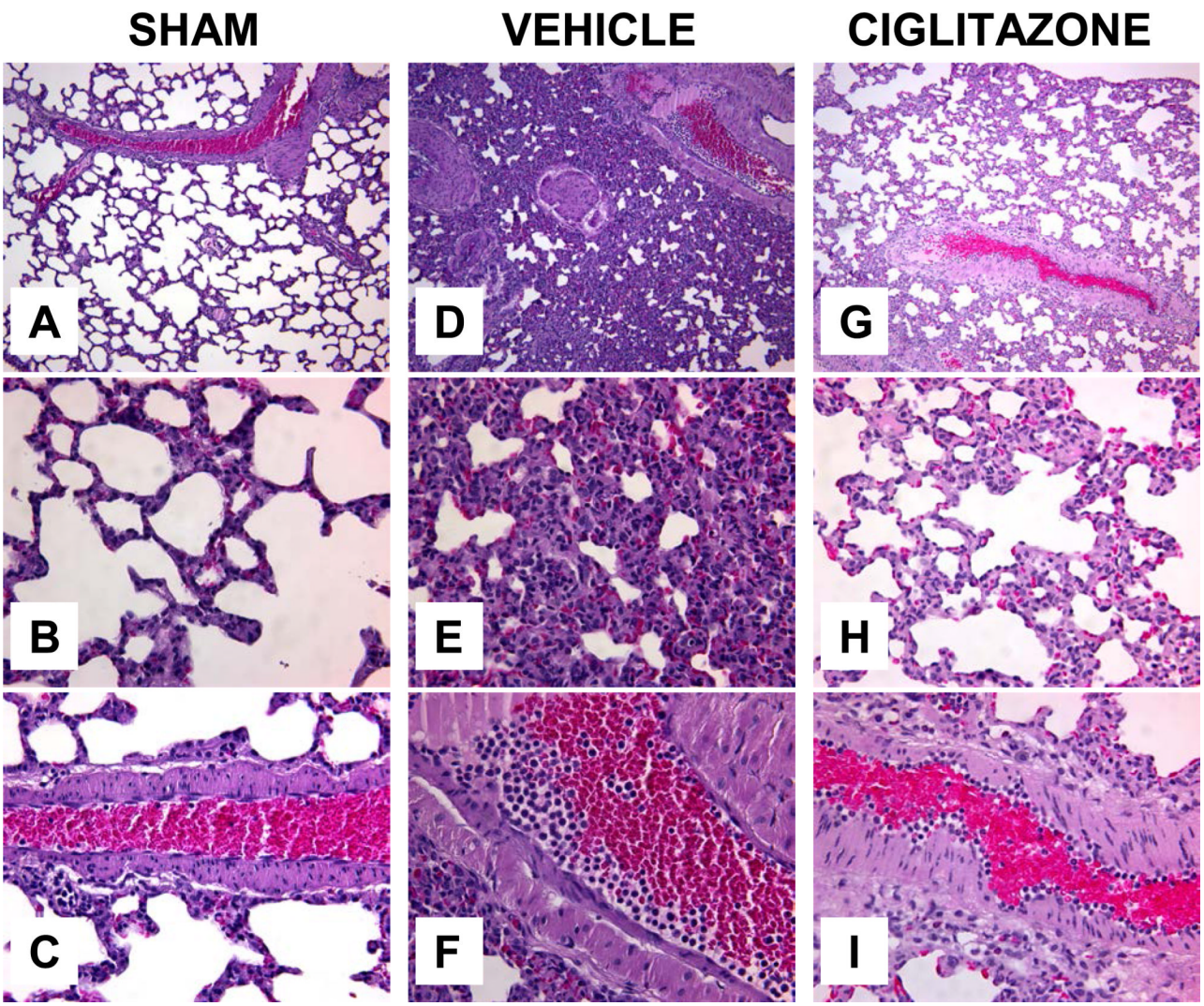

Figure 4. Effect of *in vivo* treatment with vehicle (DMSO) or ciglitazone on lung histology at 3h after resuscitation

(A) Representative photomicrograph of histology showing normal lung architecture from a sham rat (magnification 100×). (B) Representative photomicrograph of histology showing normal alveolar architecture from a sham rat (magnification 400×). (C) Representative photomicrograph of histology showing a normal lung blood vessel from a sham rat (magnification 400×). (D) Representative photomicrograph of histology showing disruption of lung architecture in a vehicle-treated rat (magnification 100×). (E) Representative photomicrograph of histology showing alveolar damage with inflammatory cell infiltration in a vehicle-treated rat (magnification 400×). (F) Representative photomicrograph of histology showing a lung blood vessel in a vehicle-treated rat (magnification 400×). (G) Representative photomicrograph of histology showing amelioration of lung architecture in a ciglitazone-treated rat (magnification 100×). (H) Representative photomicrograph of histology showing amelioration of alveolar damage and attenuation of inflammatory cell infiltration in a ciglitazone-treated rat (magnification 400×). (I) Representative photomicrograph of histology in a lung vessel in a ciglitazone-treated rat (magnification 400×). Similar histology was seen in different tissue sections (n= 3-5) in each experimental group.

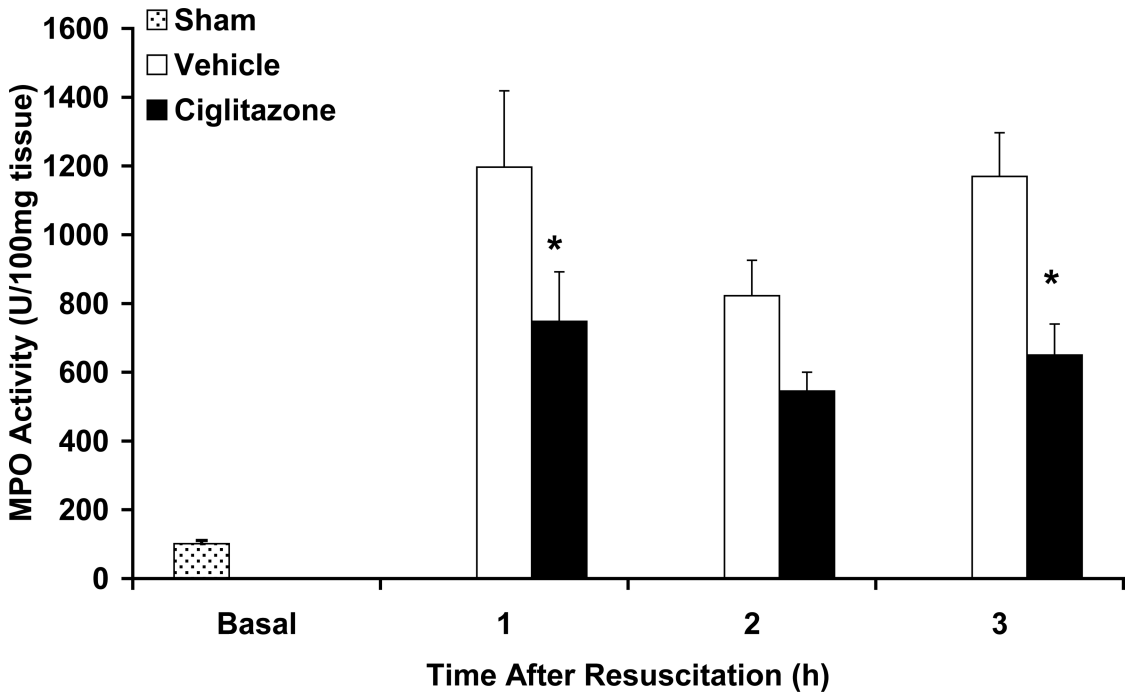

Figure 5. Effect of *in vivo* treatment with vehicle (DMSO) or ciglitazone on lung myeloperoxidase activity in rats subjected to hemorrhage and resuscitation

Each data point represents the mean ± SEM of 3 to 5 rats. Basal level represents level in sham rats, $*p < 0.05$ vs. vehicle-treated rats.

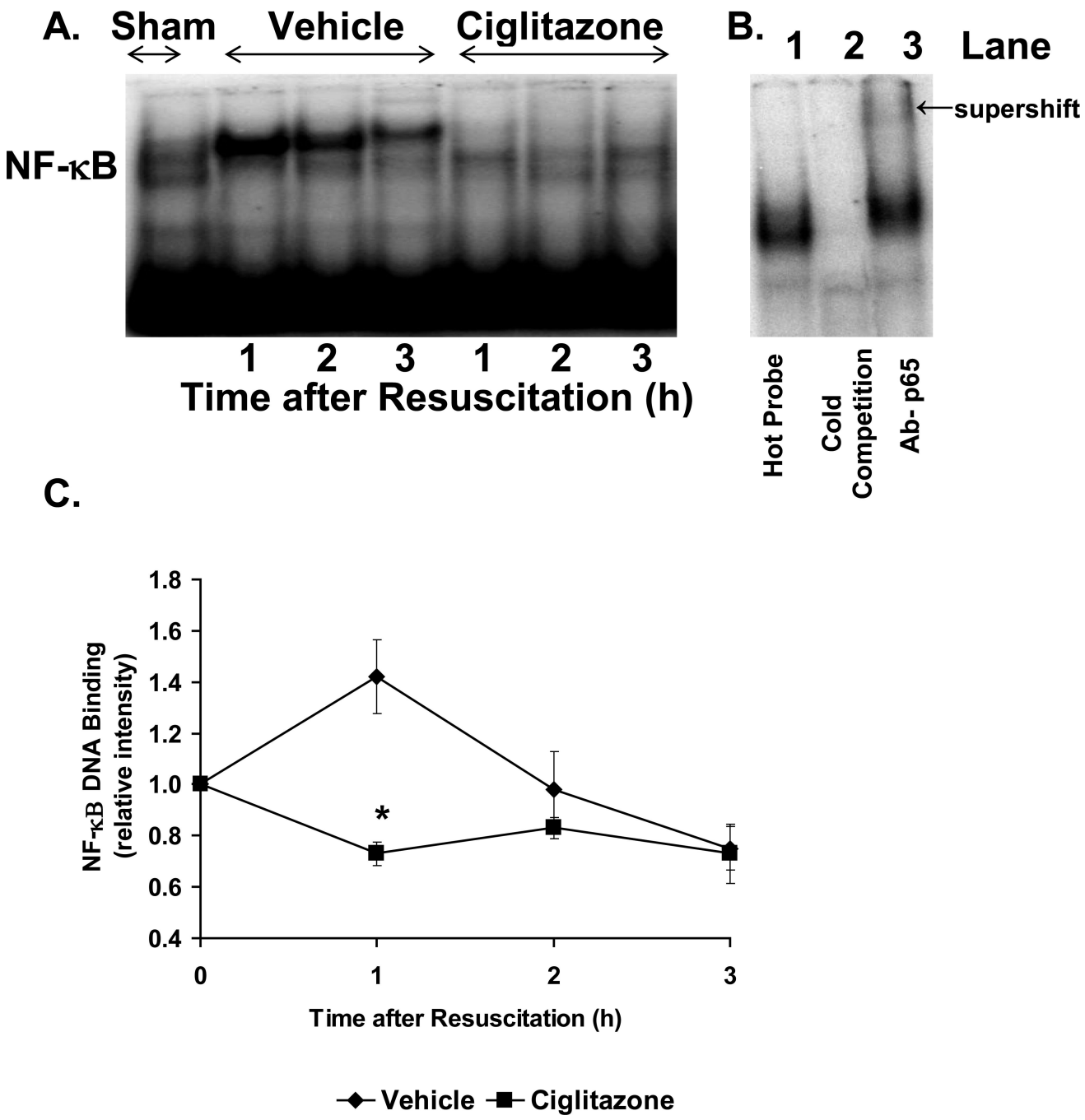

Figure 6. Effect of *in vivo* treatment with vehicle (DMSO) or ciglitazone on NF-κB DNA binding in lung

(A), Representative autoradiograph of EMSA for NF-κB; (B), Representative autoradiograph of EMSA with cold competition and supershift, *Lane 1* represents hot probe, *Lane 2* represents cold competition, *Lane 3* represents supershift with antibody to p65; (C), image analysis of activation of NF-κB determined by densitometry. The fold increase was calculated vs. the respective sham value (time zero), which was set at 1.0. Each data point represents the mean ± SEM of 3 to 5 rats. *$p < 0.05$ vs. vehicle-treated rats.

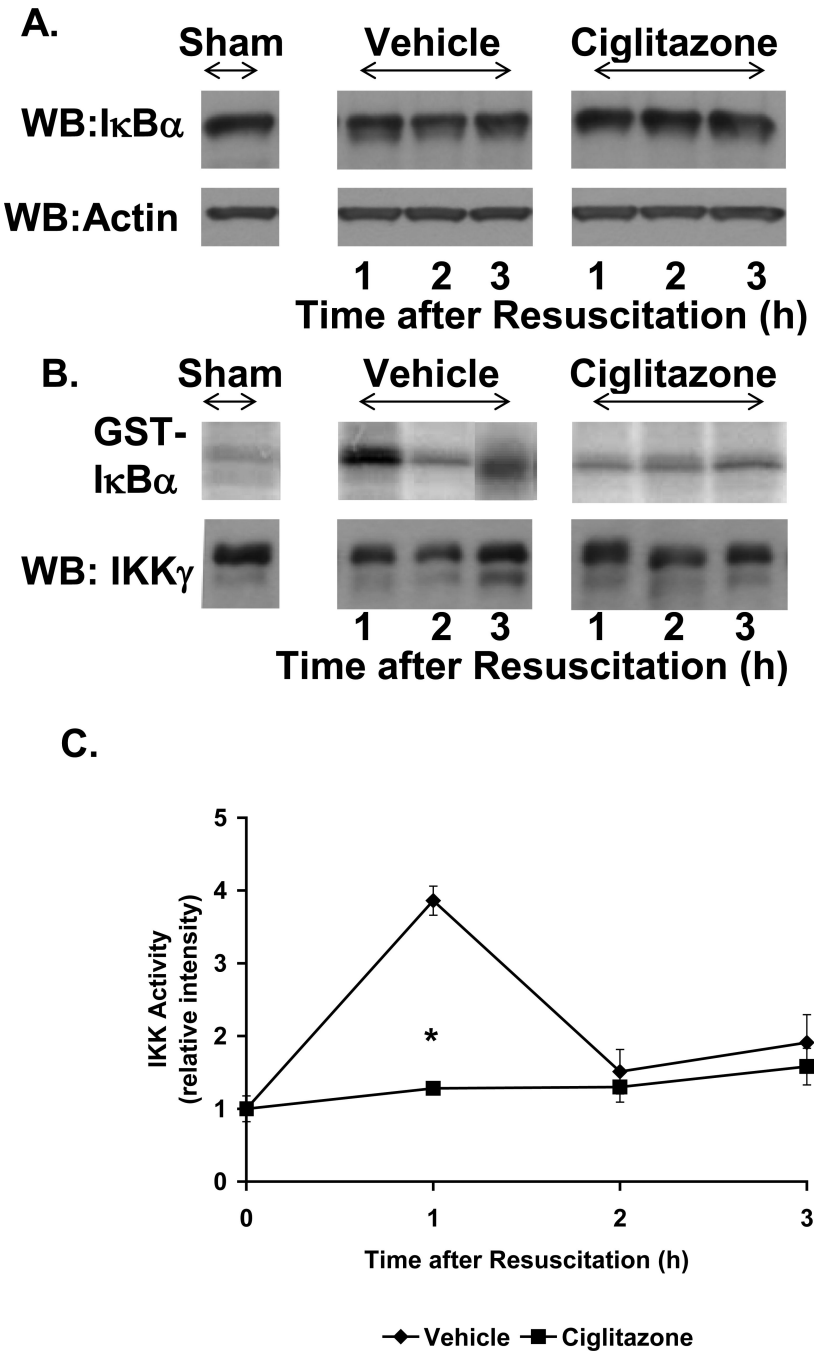

Figure 7. Effect of *in vivo* treatment with vehicle (DMSO) or ciglitazone on IκBα degradation and activation of IKK activity in the lung

(A), Representative western blot of IκBα and actin (B), Representative radiograph of IKK activity and western blot of IKKγ (C), image analysis of enzymatic activity determined by densitometry. IKK activity was estimated as the ability to phosphorylate GST- IκBα after immunoprecipitation of proteins with specific anti-IKKγ Ab. The fold increase was calculated vs. the respective sham value (time zero), which was set at 1.0. Each data point represents the mean ± SEM of 3 to 5 rats. *$p < 0.05$ vs. vehicle-treated rats.

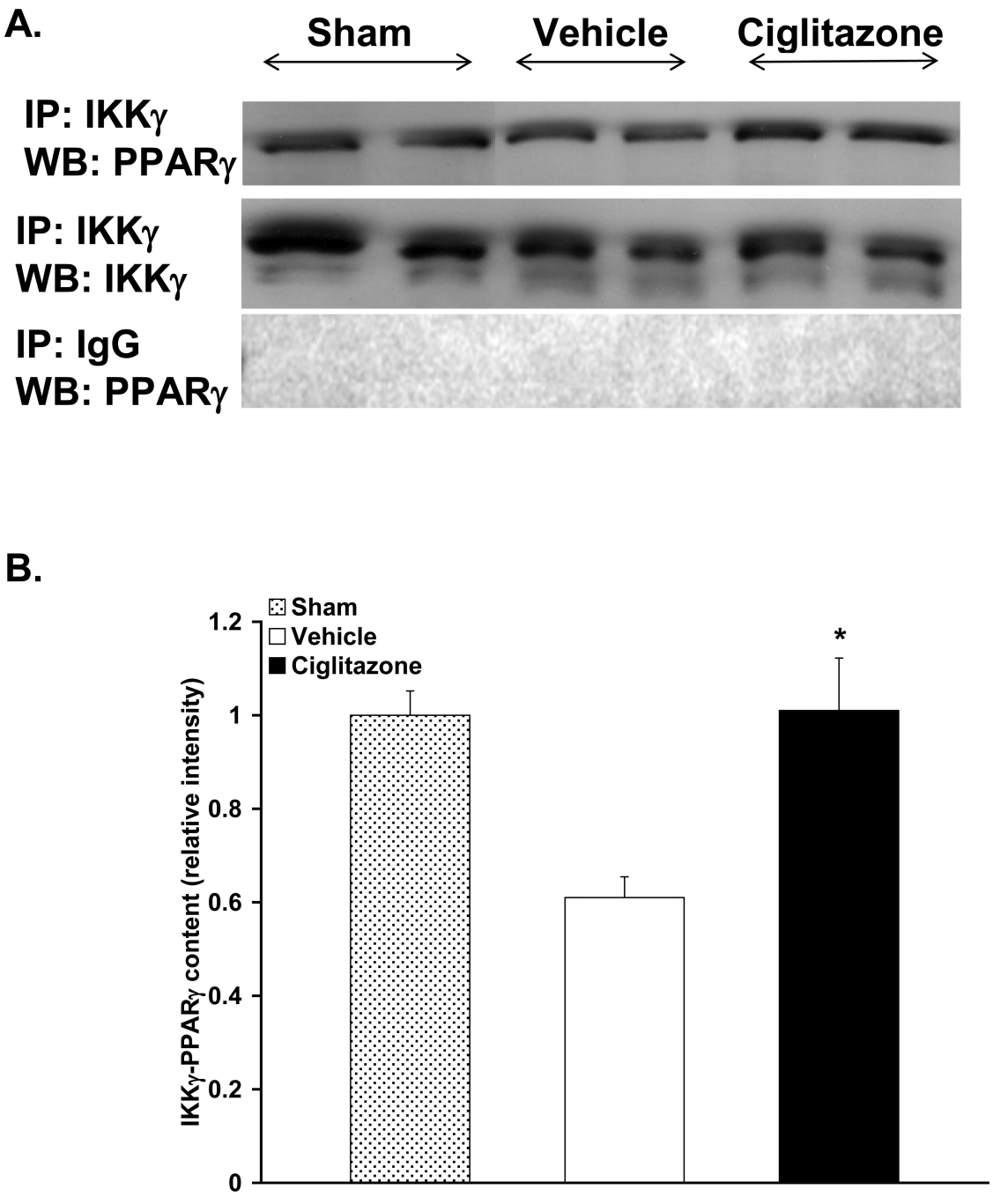

Figure 8. Effect of *in vivo* treatment with vehicle (DMSO) or ciglitazone on IKK and PPARγ Interaction in the Lung

(A), *Top,* Representative radiograph of specific immunoprecipitation study; cytosol extracts were immunoprecipitated with antibodies against IKKγ (immunoprecipitation, IKKγ) and subsequently probed with anti-PPARγ antibody (Western blot, PPARγ). *Middle,* Representative radiograph of immunoprecipitation study to assess loading; cytosol extracts were immunoprecipitated with antibodies against IKKγ (immunoprecipitation, IKKγ) and subsequently probed with antibody against IKKγ (Western blot, IKKγ). *Bottom,* Representative radiograph of control immunoprecipation study; cytosol extracts were immunoprecipitated with nonspecific preimmune goat serum (immunoprecipitation, goat

IgG) and subsequently probed with anti-PPARγ antibody (Western blot, PPARγ). (B), Image analysis of IKKγ/PPARγ interaction at 1h following resuscitation by densitometry (n=3 rats in sham and vehicle group, n=4 rats in ciglitazone group, data from 2 separate experiments). Sham was set at 1.0. *$p < 0.05$ vs. vehicle-treated rats.